FULL PAPER

# Fabrication of Silk Microneedles for Controlled-Release Drug Delivery

*Konstantinos Tsioris, Waseem K. Raja, Eleanor M. Pritchard, Bruce Panilaitis, David L. Kaplan, and Fiorenzo G. Omenetto**

**Microneedles are emerging as a minimally invasive drug delivery alternative to hypodermic needles. Current material systems utilized in microneedles impose constraints hindering the further development of this technology. In particular, it is difficult to preserve sensitive biochemical compounds (such as pharmaceuticals) during processing in a single microneedle system and subsequently achieve their controlled release. A possible solution involves fabricating microneedles systems from the biomaterial silk fibroin. Silk fibroin combines excellent mechanical properties, biocompatibility, biodegradability, benign processing conditions, and the ability to preserve and maintain the activity of biological compounds entrained in its material matrix. The degradation rate of silk fibroin and the diffusion rate of the entrained molecules can be controlled simply by adjusting post-processing conditions. This combination of properties makes silk an ideal choice to improve on existing issues associated with other microneedle-based drug delivery system. In this study, a fabrication method to produce silk biopolymer microstructures with the high aspect ratios and mechanical properties required to manufacture microneedle systems is reported. Room temperature and aqueous-based micromolding allows for the bulk loading of these microneedles with labile drugs. The drug release rate is decreased 5.6-fold by adjusting the post-processing conditions of the microneedles, mainly by controlling the silk protein secondary structure. The release kinetics are quantified in an in vitro collagen hydrogel model, which allows tracking of the model drug. Antibiotic loaded silk microneedles are manufactured and used to demonstrate a 10-fold reduction of bacterial density after their application. The processing strategies developed in this study can be expanded to other silk-based structural formats for drug delivery and biologicals storage applications.**

## 1. Introduction

Transdermal administration represents a useful route for drug and vaccine delivery due to the ease of access and avoidance of macromolecular degradation in the gastrointestinal tract. Microneedles are evolving as a safe and pain-free alternative[1] to the widely adopted skin delivery via hypodermic needles. Microneedles can be efficient, easily applied, and relatively painless, but currently face limitations due to a lack of appropriate biomaterials, an inability to precisely control the release kinetics of drugs, harsh processing conditions that limit the types of drugs that can be delivered, larger drug dose delivery, and the onset of local infections at the needle–skin interface. Options to overcome these limitations would open up new therapeutic utility for microneedle devices.

One current microneedle technology utilizes a dissolvable poly(lactide-*co*-glycolide) (PLGA) polymer microneedle body loaded with microparticles (either PLGA or carboxymethylcellulose) filled with the drug of interest to provide sustained drug release.[2] However, the fabrication method for this microneedle system constitutes a limitation, as polymer melting temperatures above 135 °C and vacuum are necessary for processing and these conditions can be detrimental to various temperature-sensitive drugs, particularly peptides and proteins. Recently developed microneedle systems employ room-temperature processing by coating solid metallic microneedle structures with polymer (a blend of carboxymethylcellulose, Lutrol F-68NF and D-(+)-trehalose dehydrate) containing an influenza vaccine.[3] The mild processing conditions resulted in some preservation of the activity of the incorporated vaccine during processing and storage over 2 to 4 weeks.[4,5] However, the coating approach to microneedle drug loading provides only a small volume to entrap therapeutic substances compared to bulk loaded structures. In addition, metal-based microneedle systems have limitations that compromise their function, such as the risk of breaking if improperly applied[6] and the possibility of an inflammatory response or infection if small metal structures remain in the skin.

The limitations described above can be addressed by fabricating bulk loaded microneedles from biocompatible and dissolvable materials like polyvinylpyrrolidone (PVP) and carbohydrates.[3,7] Relatively large doses can be administered due to the bulk loading of this dissolvable system and drug degradation

K. Tsioris, Dr. W. K. Raja, Dr. E. M. Pritchard, Dr. B. Panilaitis, Prof. D. L. Kaplan, Prof. F. G. Omenetto
Tufts University
Department of Biomedical Engineering
4 Colby St. Medford MA, 02155, USA
E-mail: Fiorenzo.Omenetto@Tufts.edu

DOI: 10.1002/adfm.201102012

caused by elevated temperatures during processing is avoided, since the polymers are cured at room temperature. However, curing requires ultraviolet light, which can impact the incorporated drug. In addition, the rapid dissolution of the microneedles provides limited control over drug release kinetics other than relatively short-term burst delivery. Previously fabricated microneedle arrays from silk protein also exhibited rapid, uncontrolled burst release.[8]

To move microneedle systems to more complete utility as a new drug delivery mode, these systems require materials that are mechanically robust,[9] biocompatible, exhibit controllable drug-release behavior, and degrade to non-toxic products in vivo within a prescribed lifetime after application.[7] Microneedle systems should also employ mild processing conditions to avoid the degradation of incorporated drugs while also promoting the stabilization of the incorporated drugs or vaccines to preserve efficacy during storage until use. Towards this need, we propose an approach that can overcome all of the established barriers, while also adding new functions to such microneedle systems, such as stabilization of the drugs in the device and programmable degradability from days to weeks. Further, since drugs such as antibiotics can be stabilized in the materials, control of infections at the site of use provides an added benefit to this technology. The proposed microneedle system combines mild fabrication conditions and controllable slow release drug delivery in a single device.

Silk fibroin has recently been shown to be a material suitable for biomedical applications due to its excellent biocompatibility and biodegradability.[10,11] Enzymes or drugs can be incorporated into the silk matrix due to the all-aqueous and mild processing conditions.[12,13] Additionally, nano- and microfabrication with silk at room temperature and atmospheric pressure has been demonstrated.[14–17] Furthermore, bioactive species have been stabilized in dry silk films for extended periods of time[12] and can be released in a controlled fashion.[18–21] Due to these properties, silk is a suitable biomaterial for bulk microneedle devices for transdermal drug delivery systems. In addition, silk outperforms other biopolymers utilized in microneedles in terms of mechanical properties.[10,11,22,23] Consequently, silk provides the necessary mechanical strength for functional microneedle devices.

We anticipate that silk microneedle systems could be exploited to meet a range of urgent clinical needs, including sustained delivery of peptide therapeutics and vaccines with short half-lives.[24] In particular, human growth hormone therapy[25,26] and vaccines requiring long-term exposure[27] would benefit from this delivery system. The stabilizing effect silk has been shown to exert on incorporated proteins could be combined with the convenience and self-administration of microneedles to produce drug delivery platforms that are safe and easy to self-administer and that can be stored at elevated temperatures.

We report on a fabrication method to produce silk biopolymer microstructures with the high aspect ratios required to manufacture microneedle systems. Room temperature and aqueous-based micromolding allow for the bulk loading of these microneedle structures with temperature-sensitive drugs such as peptides, antibiotics and vaccines, or any temperature-labile therapeutic. Additionally, we demonstrate loading of silk microneedles with various model drugs, as well as with antibiotic. Controlled release of a model drug is achieved by adjusting the post-processing conditions of the microneedle structures, mainly by controlling the silk protein secondary structure. A collagen hydrogel-based in vitro skin model allows quantification of the varied drug release profiles, as they are demonstrated in this study.

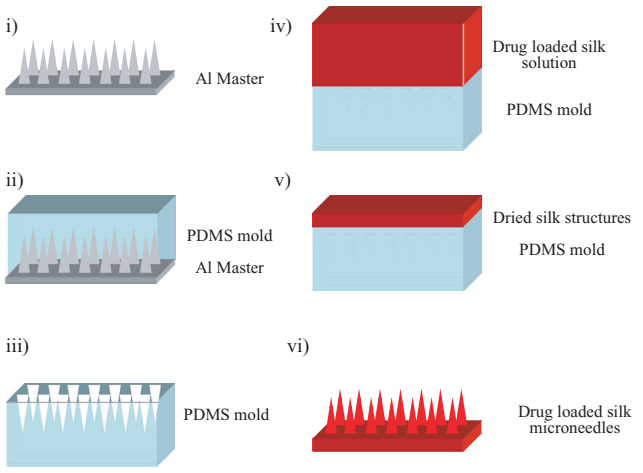


**Figure 1.** Drug-loaded silk microneedles fabrication process: i) Al master is manufactured by high speed milling and chemical wet etching, ii) PDMS is cast over Al master to produce negative mold, iii) PDMS mold is removed from Al master, iv) drug-loaded silk solution is cast over PDMS mold, v) silk is allowed to dry, and, vi) drug-loaded silk microneedles are removed from PDMS mold.

## 2. Fabrication Strategy for Silk Microneedles

**Figure 1** illustrates the process to fabricate silk microneedles. The effectiveness of this technique is demonstrated by micromolding silk microneedles at ambient pressure and temperature. The aqueous derived silk microneedles reproduce faithfully the molding master, are approximately 500 micrometers high, with tip radii of less than 10 μm and are doped with the horseradish peroxidase (HRP) enzyme, to use as a large molecule model drug. In addition, separate silk microneedles were loaded with the antibiotic tetracycline. For the purposes of visualization, we incorporated reactive red 120 dye into the silk microneedles depicted in **Figure 2**.

The aluminum (Al) microneedle molding masters were fabricated in a high speed micromilling approach followed by isotropic wet etching. The milling step provides rudimentary microneedle templates with dimension that approximate the desired topology while the timed chemical etching of the Al templates refines the structure, yielding a needle array of approximately 500 μm needle height and tip radii of less than 10 μm. These Al microneedle masters were used to fabricate an elastomer-based microneedle negative mold using polydimethylsiloxane (PDMS) by using established soft lithography techniques.[28] Employing this soft elastomer material allows us to faithfully reproduce micron-scale features and easily detach the silk structures while minimizing the probability of damaging the resulting devices.[19] Furthermore, the surface properties of PDMS can be modified from hydrophobic to partially

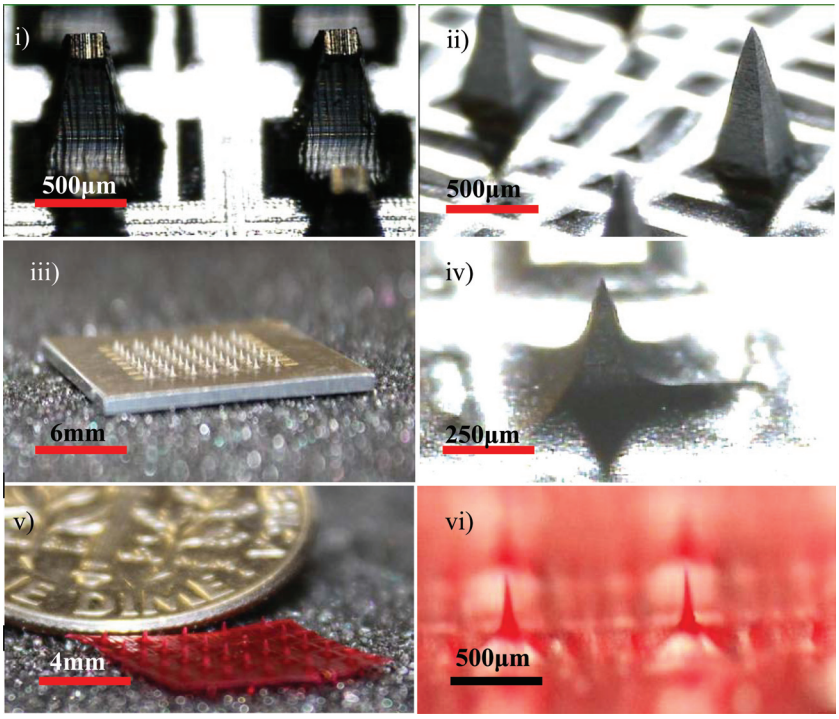


**Figure 2.** Images of Al molding master and silk microneedles: i) Al needle template after mechanical milling, ii) Al microneedle master after 20 min of chemical etching, iii) macroscopic view of Al microneedle master, iv) Al microneedle master after 2 h of chemical etching, v) macroscopic view of drug-loaded silk microneedle patch, and, vi) drug-loaded silk microneedles.

hydrophilic by briefly exposing the elastomer surface to oxygen plasma.[29] In addition, the porous network of PDMS allows removal of water through the elastomer.[30] These are essential characteristics to obtain high aspect ratio silk structures in the molding process.

Aqueous silk solution (6%–8% w/v) was cast over the treated PDMS template. The silk solution transitions to the solid-state by overnight drying and the silk microneedle array can be then detached from the PDMS mold.[22] The resulting silk microneedles can be further modified by post-processing to adjust the degradation rate and diffusion properties. This degree of control is achieved by adjusting the protein secondary structure. A high content of beta sheet secondary structure renders the silk films water insoluble. The beta sheet content can be controlled by adjusting the hydration state of the silk material[22] through its drying rate,[31] exposure to methanol or high humidity (e.g., water vapor annealing), or various temperature, mechanical, and electrical exposures.[22,31–33] Adjusting the amount of beta sheet content yields silk materials with controlled crystallinity, solubility and release kinetics.[32–35] We selected various water vapor annealing times to adjust the silk microneedle drug-release properties. These post-processing steps allow control over the diffusivity of the silk microneedles, ultimately providing control over drug release kinetics.

Furthermore, we demonstrated mechanical functionality of the silk microneedle system in a mouse skin model (**Figure 3**). Silk microneedle patches were prepared as described above and applied to mouse skin (see the Experimental Section). Silk microneedles successfully breached the epidermis to access the underlying tissue. This demonstrates that silk microneedles provide sufficient mechanical strength to penetrate skin for the delivery of pharmaceuticals.

## 3. Tissue Model for Quantification of Microneedles Release Kinetics

To quantify the release kinetics of silk microneedles, a gelatin hydrogel and polymer film membrane construct was used (**Figure 4**). This in vitro model provides improved experimental control compared to in vivo or cadaver skin models. A 10–20% gelatin hydrogel was selected due to its common use as a tissue analog in ballistic testing.[36] In addition, collagen hydrogels are optically transparent allowing assessment of the release kinetics. Furthermore, the water content, diffusion and mechanical properties of the collagen hydrogels can also be adjusted. The polymer membrane has a dual purpose in simulating the outer layer of the skin to demonstrate successful piercing of the membrane for adequate mechanical toughness of the needles and to function as a diffusion barrier to prevent the microneedles' bulk silk substrate from releasing the model drug into the underlying collagen hydrogel (i.e., to ensure that the monitored release is from the needles alone).[37,38] The polymer membrane was first placed over the HRP loaded microneedles patch followed by application to the collagen slab, as shown in Figure 4.

## 4. Controlled-Release and Activity Preservation of an Enzymatic Model Drug

**Figure 5** depicts the enzymatic activity of the HRP, which retained activity during silk processing and collagenase digestion and was detected by using a chromogenic substrate (see the Experimental Section) which turns blue in the presence of active HRP. The release kinetics of HRP from silk microneedles into the collagen hydrogels ($N = 3$) were determined spectroscopically. The collagen hydrogel was selectively digested with collagenase. Subsequently, a colorimetric HRP enzyme activity assay was carried out (see the Experimental Section) (Figure 5). The insert in Figure 5 shows the initial HRP release in collagen hydrogels. A sustained release of HRP was observed over the entire test period. The maximum release of 54 pg of HRP per needle after 48 h was observed in the untreated microneedles devices. Compared to the 2 and 8 h water-annealed devices, the untreated silk microneedles released in the same time period $2.7 \pm 0.18$ and $5.6 \pm 0.99$ times as much HRP, respectively. The beta sheet content in the samples was determined as previous described by infrared spectroscopy[33] with results of 14%, 18% and 21% for the untreated, 2 h annealed, and 8 h annealed samples, respectively. As expected, the increased water vapor

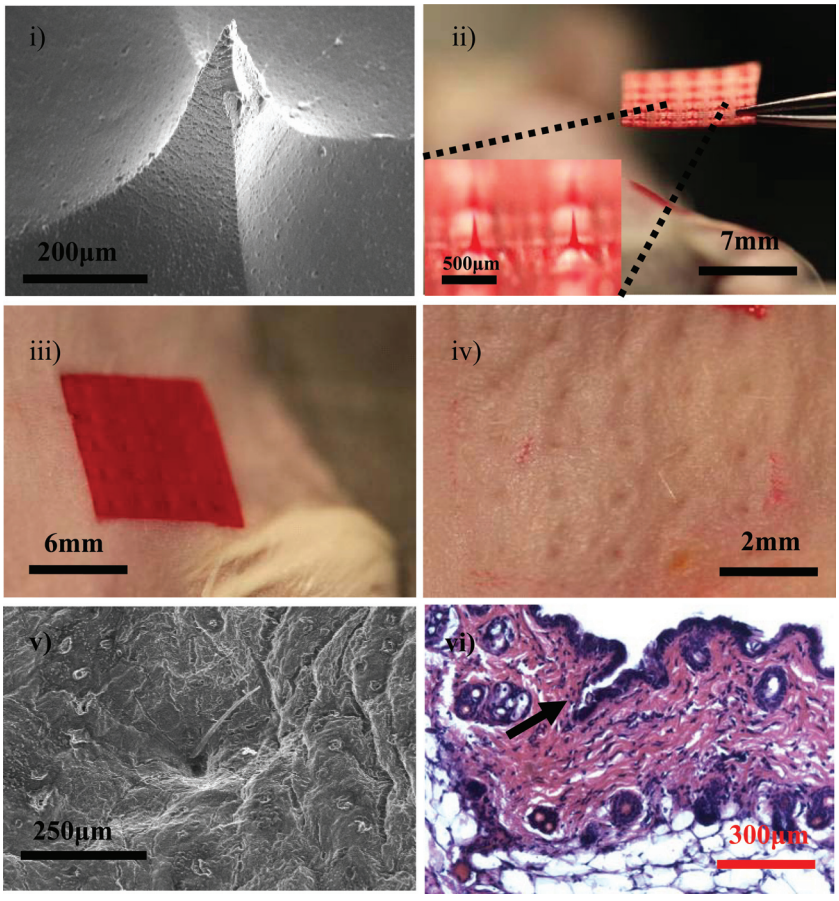


**Figure 3.** Silk microneedles as applied to mouse skin: i) scanning electron micrograph of an individual silk microneedle, ii) silk microneedles patch, relative size comparison to mouse, iii) silk microneedles patch applied to animal skin, iv) skin after removal of microneedles patch, needle penetration marks are clearly visible, v) scanning electron micrograph of penetrated skin, and, vi) histology section of individual indentation site – epidermis was breached (arrow) allowing access to the underlying tissue; Successful penetration of skin demonstrates sufficient mechanical strength of silk microneedles.

annealing time increased beta sheet content and reduced HRP release offering a way to control release. The quantified drug release in this study was determined for single needles. Delivery of larger doses can easily be achieved by scaling the microneedles patch size and needle density.

## 5. Pathogen Reduction Through Delivery of Antibiotics with Silk Microneedles

Furthermore, to demonstrate the potential to reduce infections with microneedles, antibiotic-loaded silk microneedles were prepared and assessed. Tetracycline-loaded and plain silk microneedles (used as controls) were prepared as described above. The silk microneedles arrays were used as discussed in Figure 4 (only the microneedles are exposed) and affixed to the bottom of a cell culture plate using PDMS. Tryptic Soy Agar was added to each plate containing either loaded or unloaded microneedles arrays and allowed to gel. Subsequently *Staphylococcus aureus* bacteria were applied to each plate and incubated overnight at 37 °C to allow the formation of a bacterial lawn.

Tetracycline-releasing microneedles resulted in a visible decrease in bacterial density in the region of drug release (**Figure 6**a). To quantify bacterial density, the 10 mm diameter region of agar above the microneedle arrays was excised, homogenized in culture broth and plated in triplicate. The plated liquid cultures were incubated overnight at 37 °C to allow colony growth. A 10-fold decrease in colony forming units (in million CFU per excised ear) for samples exposed to drug loaded microneedles was found relative to the controls (Figure 6b). The antibiotic-loaded microneedles inhibited the growth of bacteria.

## 6. Conclusions

The fabrication of high-aspect-ratio silk microneedles was demonstrated. Due to the mild processing conditions of this method and the favorable properties of the silk biomaterial, sensitive drugs (such as antibiotics, as well as labile enzymes) can be incorporated and stored in the microneedles. Additionally, we demonstrated controlled release of a large molecule from post-treated microneedles fabricated entirely under mild ambient conditions, thereby preserving function. Lastly, microneedles loaded with antibiotics inhibit the growth of pathogens and offer an attractive strategy to prevent local infections. The silk-based microneedle systems presented

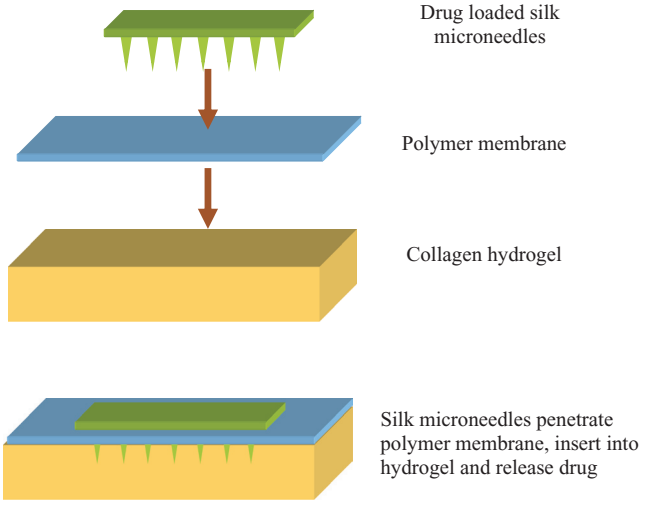


**Figure 4.** Scheme describing experimental setup to test drug-loaded silk microneedles in an in vitro hydrogel skin model. Silk microneedles penetrate polymer membrane and collagen hydrogel to subsequently release model drug in a controlled fashion.

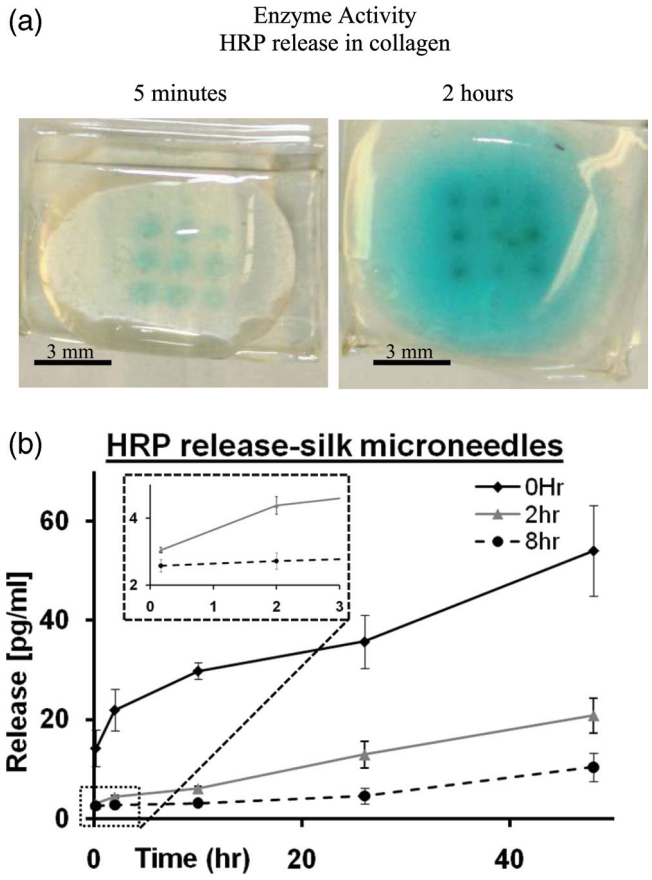


**Figure 5.** a) Bioactivity of microneedle released HRP into the collagen slab after 5 min and 2 h release was detected by chromogenic substrate. b) Total model drug release of silk microneedles in collagen hydrogels, as determined from collagenase digestion and absorption spectroscopy with the insert depicting the early events of release ($N = 3$, error bars represent standard deviations).

here are an example of recapitulation of form and function, successfully addressing current limitations associated with other polymeric or metallic microneedle systems and providing an effective path for storage and delivery of drugs and therapeutics. Furthermore, the strategies developed in this study can be expanded into other silk-based structural formats for drug delivery and biologicals storage applications.

## 6. Experimental Section

*Master Mold Fabrication*: The Al master was fabricated by computer numerical control CNC machining with a 0.5 mm, 15° end mill, in a custom made 70k rpm tool. The Al template was further processed by a timed (1.5 h) chemical wet etch in Al etchant at 50° (Al etchant type A, 80% phosphoric acid, 5%, nitric acid, 5% acetic acid, and 10% distilled water).

*Silk Extraction*: The process to obtain aqueous silk fibroin solution from *Bombyx mori* cocoons was previously described.[39] Briefly, sericin was removed by boiling the cocoons in an aqueous sodium carbonate solution for 40 min. After drying, the fibroin fibers were dissolved in lithium bromide solution and subsequently the salt was removed by dialysis against deionized (DI) water until the solution reached a concentration of about 6–8% w/v.

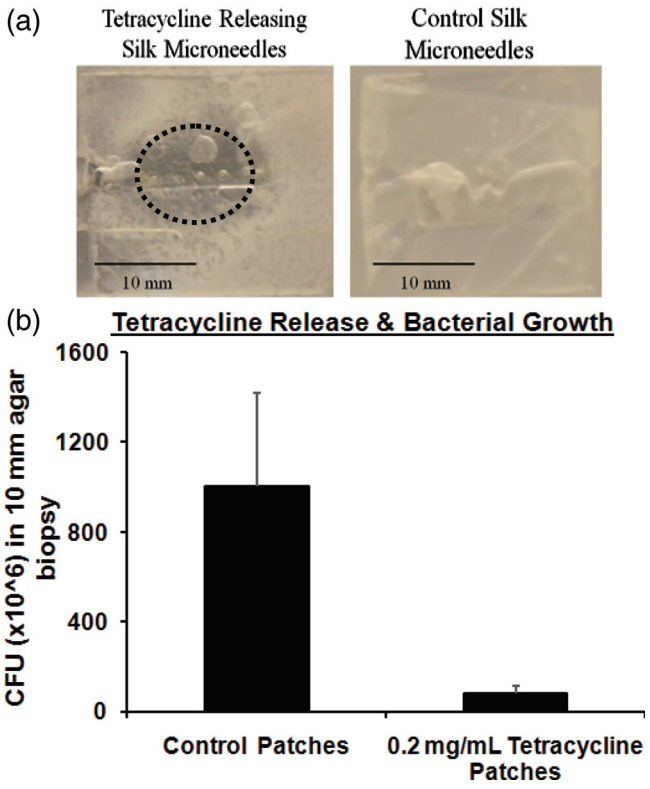


**Figure 6.** a) Representative photographs of the zones of clearance in *S. aureus* lawns exposed to tetracycline-loaded silk microneedles and control silk microneedles. b) Average colony forming unit (CFU) counts for *S. aureus* lawns exposed to tetracycline-loaded and control silk microneedles in $10^6$ CFU per 10 mm diameter agar biopsy sample ($N = 3$, error bars represent standard deviations).

*Silk Microneedles Skin Penetration*: The mouse was anesthetized using a standard ketamine and xylazine mix (ketamine 90–120 mg $kg^{-1}$; xylazine 10 mg $kg^{-1}$). The skin was shaved and the remaining hair removed with a commercial hair remover (Nair; Church & Dwight Co., Inc., Princeton, NJ). The skin was cleaned, removed from the animals, placed in wet gauze to stay hydrated and used within 2 h. The silk microneedles patches were either directly applied on the mouse for 30 min or were placed onto the cadaver skin for 5 min. The cadaver skin was placed on 10 to 12 layers of tissue papers to mimic a tissue-like mechanical environment.[40] For scanning electron microscopy, the samples were fixed in 3% glutaraldehyde and subsequently coated with gold/platinum. For histology, the microneedles treated skin was fixed in formaldehyde (10%) for 24 h, and subsequently embedded in paraffin wax. A microtome was used to prepare 10 µm thick slices. The slices were stained with hematoxylin eosin (H&E) staining and imaged with a brightfield microscope. All animal studies were performed under protocols approved through the Tufts University IACUC.

*Release Model*: The silk microneedles were loaded with 1 mg $mL^{-1}$ of HRP (Sigma–Aldrich). The silk microneedle patches were treated by water vapor annealing for 2 and 8 h to modify the release characteristics. Gelatin hydrogel was prepared by boiling 40 mL DI water and mixing it with 4.5 g of Knox™ original unflavored gelatin powder to obtain 0.112 g $mL^{-1}$ concentration hydrogel. The solution was poured into a 100 mm diameter Petri dish and allowed to cool. The collagen slab measured approximately 2.5 mm in height. The slabs were cut into 10 mm × 5 mm sections. The silk microneedle patches were diced into 2 needle arrays. The needles were pierced through Parafilm (Parafilm M, Pechiney Plastic Packaging) membranes and subsequently applied to the hydrogel slabs to quantify the HRP release. All constructs were

kept in a humid environment to avoid dehydration of the hydrogels. To quantify the total amount of HRP release from the silk microneedles, stacks of silk microneedles, polymer membranes, and collagen hydrogels were prepared and evaluated at multiple time points. Once each time point was reached, the microneedles were removed from the hydrogel slab to stop further release of HRP. The hydrogel slabs were digested in 400 µL of 1 mg $mL^{-1}$ collagenase (Sigma–Aldrich) for 2 h at 36 °C. Subsequently, HRP content was quantified according to protocol using TMB Peroxidase substrate (Bethyl Laboratories Inc). Briefly, the two substrate components (0.4 g $L^{-1}$ solution of 3,3′,5,5′-tetramthylbenzidine (TMB) and a 0.02% solution of $H_2O_2$ in citric acid) were brought to room temperature, mixed in equal volumes, and added to samples containing HRP (including standards and experimental samples). Samples were incubated at room temperature for approximately 5–10 min until sufficient color change was observed, then an equal volume of $H_2SO_4$ was added to stop color development. Absorbance was read with a microplate reader at a wavelength of 450 nm. Concentration standards were prepared under the same conditions in parallel.

*Fourier-Transform Infrared (FTIR) Spectroscopy*: FTIR measurements (FT/IR-6200 Spectrometer, Jasco) and analysis was performed as previously described.[33] Fourier self-deconvolution of the IR spectra of the amide I region was performed by OPUS 5.0 software (Bruker Optics). The deconvolution was performed with a half-bandwidth of 27 $cm^{-1}$ and a noise reduction factor of 0.3.

*Antibiotic-Loaded Silk Microneedles and Bacterial Growth*: Microneedle patches loaded with 2 mg $mL^{-1}$ tetracycline were fabricated as discussed above. Tryptic Soy Agar was prepared according to manufacturer's instructions and aliquoted into 100 mm diameter Petri dish (15–20 mL per plate). Lyophilized *S. aureus* ATCC 25923 bacteria cultures were reconstituted and expanded according to manufacturer instructions. To test susceptibility, liquid cultures were grown for 18–24 h to an optical density ($OD_{600}$) between 1 and 1.2 (corresponding to a viable count of approx. $10^6$ CFU $mL^{-1}$). A 10 mm diameter biopsy (total area approximately 78.5 $mm^2$) was used to excise the agar above the microneedle arrays. The array samples were immersed in 10 mL of Tryptic Soy Broth and homogenized for 5–10 s. The homogenate was diluted and plated on Tryptic Soy Agar plates (0.5 mL of liquid culture per plate). After liquid cultures were incubated, the lowest dilution for which individual colonies were distinguishable was selected and colonies were counted (3 plates per sample, 3 samples per treatment type).

## Acknowledgements

K.T. and W.K.R. contributed equally to this work. This material is based upon work supported in part by the U.S. Army Research Laboratory and the U.S. Army Research Office under contract number W911 NF-07-1-0618 and by the DARPA-DSO, as well as the Air Force Office of Scientific Research (FA9550-10-1-0172).

Received: August 24, 2011
Published online: December 2, 2011

[1] A. Arora, M. Prausnitz, S. Mitragotri, *Int. J. Pharm.* **2008**, *364*, 227.
[2] J. H. Park, M. G. Allen, M. R. Prausnitz, *Pharm. Res.* **2006**, *23*, 1008.
[3] S. Sullivan, D. Koutsonanos, M. del Pilar Martin, J. Lee, V. Zarnitsyn, S. Choi, N. Murthy, R. Compans, I. Skountzou, M. Prausnitz, *Natu. Med.* **2010**, *16*, 915.
[4] Y. C. Kim, F. S. Quan, R. W. Compans, S. M. Kang, M. R. Prausnitz, *J. Controlled Release* **2010**, *142*, 187.
[5] Y. C. Kim, F. S. Quan, R. W. Compans, S. M. Kang, M. R. Prausnitz, *Pharm. Res.* **2011**, *28*, 135.
[6] R. F. Donnelly, D. I. J. Morrow, T. R. R. Singh, K. Migalska, P. A. McCarron, C. O'Mahony, A. D. Woolfson, *Drug Dev. Ind. Pharm.* **2009**, *35*, 1242.
[7] S. Sullivan, N. Murthy, M. Prausnitz, *Adv. Mater.* **2008**, *20*, 933.
[8] X. You, J. J. Pak, J.-h. Chang, *Proc. IEEE, Int. Conf. on Nano/Molecular Med. and Eng.* **2010**, 144.
[9] S. Davis, B. Landis, Z. Adams, M. Allen, M. Prausnitz, *J. Biomech.* **2004**, *37*, 1155.
[10] G. Altman, F. Diaz, C. Jakuba, T. Calabro, R. Horan, J. Chen, H. Lu, J. Richmond, D. Kaplan, *Biomaterials* **2003**, *24*, 401.
[11] C. Jiang, X. Wang, R. Gunawidjaja, Y. Lin, M. Gupta, D. Kaplan, R. Naik, V. Tsukruk, *Adv. Funct. Mater.* **2007**, *17*, 2229.
[12] S. Lu, X. Wang, Q. Lu, X. Hu, N. Uppal, F. Omenetto, D. Kaplan, *Biomacromolecules* **2009**, 217.
[13] S. Lu, X. Wang, Q. Lu, X. Hu, N. Uppal, F. Omenetto, D. Kaplan, *Biomacromolecules* **2009**, *10*, 1032.
[14] J. Amsden, H. Perry, S. Boriskina, A. Gopinath, D. Kaplan, L. Dal Negro, F. Omenetto, *Opt. Express* **2009**, *17*, 21271.
[15] F. Omenetto, D. Kaplan, *Nat. Photonics* **2008**, *2*, 641.
[16] H. Perry, A. Gopinath, D. Kaplan, L. Dal Negro, F. Omenetto, *Adv. Mater.* **2008**, *20*, 3070.
[17] K. Tsioris, H. Tao, M. Liu, J. Hopwood, D. Kaplan, R. Averitt, F. Omenetto, *Adv. Mater.* **2011**, *23*, 2015.
[18] J. Chen, N. Minoura, A. Tanioka, *Polymer* **1994**, *35*, 2853.
[19] X. Y. Liu, C. C. Zhang, W. L. Xu, C. Ouyang, *Mater. Lett.* **2009**, *63*, 263.
[20] S. Putthanarat, R. Eby, R. Naik, S. Juhl, M. Walker, E. Peterman, S. Ristich, J. Magoshi, T. Tanaka, M. Stone, *Polymer* **2004**, *45*, 8451.
[21] L. Uebersax, H. Hagenmuller, S. Hofmann, E. Gruenblatt, R. Muller, G. Vunjaknovakovic, D. L. Kaplan, H. P. Merkle, L. Meinel, *Tissue Eng.* **2006**, *12*, 3417.
[22] H. Jin, J. Park, V. Karageorgiou, U. Kim, R. Valluzzi, P. Cebe, D. Kaplan, *Adv. Funct. Mater.* **2005**, *15*, 1241.
[23] A. Sionkowska, M. Wisniewski, J. Skopinska, S. Vicini, E. Marsano, *Polym. Degrad. Stab.* **2005**, *88*, 261.
[24] C. Cullander, R. H. Guy, *Adv. Drug Delivery Rev.* **1992**, *8*, 291.
[25] H. Kwak, W. Shim, M. Choi, M. Son, Y. Kim, H. Yang, T. Kim, G. Lee, B. Kim, S. Kang, *J. Controlled Release* **2009**, *137*, 160.
[26] J. W. Lee, S. O. Choi, E. I. Felner, M. R. Prausnitz, *Small* **2011**, *7*, 531.
[27] J. Kemp, M. Kajihara, S. Nagahara, A. Sano, M. Brandon, S. Lofthouse, *Vaccine* **2002**, *20*, 1089.
[28] D. B. Wolfe, D. Qin, G. M. Whitesides, *Methods Mol. Biol.* **2010**, *583*, 81.
[29] S. Bhattacharya, A. Datta, J. M. Berg, S. Gangopadhyay, *J. Microelectromech. Syst.* **2005**, *14*, 590.
[30] L. Fritz, D. Hofmann, *Polymer* **1997**, *38*, 1035.
[31] Q. Lu, X. Hu, X. Wang, J. A. Kluge, S. Lu, P. Cebe, D. L. Kaplan, *Acta Biomater.* **2010**, *6*, 1380.
[32] S. Hofmann, C. Wong Po Foo, F. Rossetti, M. Textor, G. Vunjak-Novakovic, D. Kaplan, H. Merkle, L. Meinel, *J. Controlled Release* **2006**, *111*, 219.
[33] X. Hu, D. Kaplan, P. Cebe, *Macromolecules* **2006**, *39*, 6161.
[34] E. M. Pritchard, C. Szybala, D. Boison, D. L. Kaplan, *J. Controlled Release* **2010**, *144*, 159.
[35] X. Wang, X. Hu, A. Daley, O. Rabotyagova, P. Cebe, D. L. Kaplan, *J. Controlled Release* **2007**, *121*, 190.
[36] G. Wightman, J. Beard, R. Allison, *Forensic Sci. Int.* **2010**, *200*, 41.
[37] B. Forslind, M. Lindberg, G. M. Roomans, J. Pallon, Y. Werner-Linde, *Microsc. Res. Tech.* **1997**, *38*, 373.
[38] W. Montagna, P. F. Parakkal, *The Structure and Function of Skin*, Academic Press, New York **1974**.
[39] S. Sofia, M. B. McCarthy, G. Gronowicz, D. L. Kaplan, *J. Biomed. Mater. Res.* **2001**, *54*, 139.
[40] J. H. Park, M. G. Allen, M. R. Prausnitz, *J. Controlled Release* **2005**, *104*, 51.